Paper: ASAT-17-045-TH

17th International Conference on
AEROSPACE SCIENCES & AVIATION TECHNOLOGY,
ASAT - 17 – April 11 - 13, 2017, E-Mail: asat@mtc.edu.eg
Military Technical College, Kobry Elkobbah, Cairo, Egypt
Tel: +(202) 24025292 – 24036138, Fax: +(202) 22621908

Numerical Investigation of Film Cooling over a Flat Plate with Varying Injection Angle

Abdelaziz Elareibi*, Tarek Elnady†, Ali Elmaihy‡, Salman Elshmarka§

Abstract: Numerical investigations have been conducted in order to find appropriate turbulence model and near wall treatments to study the effect of injection angle. For this purpose, different turbulence models such as k- ε models (standard, RNG and realizable), and k- ω models (standard and the Shear Stress Transport (SST) model) were examined to solve for the most convenient accurate prediction of the flow field. In addition, two different wall functions (standard wall function and enhanced two-layer wall function were tested and compered with the experimental study at two blowing ratios (0.5, 1) and two injection angles (35^o, 55^o). It was found that the realizable k–ε model with enhanced all treatment (two-layer approach) was in reasonable agreement with experimental data, which proved its advantage as compared with other turbulence models. So the realizable k–ε model with enhanced wall treatment (two-layer approach) was selected in this paper to study the effect of injection angle variation. The film cooling geometry in the present paper is similar to that used in a previous study. The coolant flow temperature was kept constant at 188 K at a velocity 6.25 m/s and a constant density ratio of 1.6. The results showed a reduction in effectiveness for the injection angle of 55^o as compared to effectiveness for the injection angle of 35^o.

Nomenclature

X	axial/stream wise coordinate, m
Y	vertical coordinate, m
Z	lateral coordinate, m
D	hole diameter
L	length of the hole, m
P	hole pitch distance, m
M	Blowing Ratio, [(pv)j/(pv)m]
T	temperature, K
k	Turbulence kinetic energy, m2/s2
ρ	Density, kg/m3
ω	Specific turbulence dissipation rate, 1/s

Subscripts

aw	adiabatic wall
m	main flow
j	jet

Greek Symbols

η	Film cooling effectiveness
ε	Turbulence eddy dissipation, m2/s3

Acronyms

DR	Density Ratio (pj/pm)

* Libyan Armed Forces, Libya.
† Egyptian Armed Forces, Egypt.
‡ Egyptian Armed Forces, Egypt; ali.elmaihy@mtc.edu.eg
§ Egyptian Armed Forces, Egypt.

1. Introduction

Film cooling is one of the widely applied cooling techniques by the gas turbine manufacturers. Film cooling is the process of ejecting coolant from a selected location, which forms a protective thermal barrier on the surface to be cooled [2]. The performance of the coolant ejected from the hole is calculated using the non-dimensional temperature term defined as local adiabatic effectiveness (η).

$$\eta = \frac{T_{aw} - T_m}{T_j - T_m} \quad (1)$$

where the subscript (m) refers to the mainstream, the subscript (j) refers to the jet coolant and the subscript (aw) refers to the adiabatic wall.

2. Literature Review

Film cooling has great importance, and widespread applications, so it has been extensively studied over the last decades. A large body of investigations has been generated relevant to film cooling. The majority of these investigations have been done on a flat surface, due to complexity in studying on a true airfoil curved surfaces of blades and vanes. The results of those investigations are considered as fundamental data to know the effect of different factors on the performance of film cooling. Focus in this paper will be on investigations related to the effects of injection angle, wall treatment, and turbulent models. Several experimental investigations have been conducted to study the film cooling performance at different injection angles. Bogard et al. [1] experimentally studied the performance of film cooling over flat plate at two different injection angles 35º and 55º for blowing ratios of M=0.5 and 1 at a density ratio of 1.6 and low free-stream turbulence of 0.2%. They noted that larger streamwise injection angles provide 10% lower film effectiveness than shallow angles at blowing ratio of 0.5. However, large angle injection provides much lower effectiveness (30% less) than shallow angles at higher blowing ratio of 1. Foster et al. [3] investigated the film cooling performance for hole injection angles of 35º and 90º. Slightly decreased in film cooling effectiveness was found for the 90° holes at M =0.5, but improved performance was found for the 90-deg holes for a high blowing ratio of M =1.4. Similar results were found by Baldauf et al.[4] who compared holes with 30^0, 60^0, and 90^0 injection angles. Their results showed about a 30% decrease in film cooling effectiveness peak values for lower blowing ratios for 90^0 injection compared to 30^0 injection.

Selection of type of wall treatments and numerical model plays role in investigating numerically the performance of film cooling. The numerical results of Amer et al. [5] for four different models showed that the two-equation turbulence models do not work well for film cooling, especially in the near-hole field and at high blowing ratios. Comparative investigations were conducted by Sarkar et al. [6] involving the k-ε and k-ω models, Baldwin Lomax, and a relaxation eddy viscosity model on a flat plate with a slot. The low-Reynolds k-ε model was found preferable for the selected application. The k-ω model performed the worst in capturing the surface temperature distribution. It was also found that the relaxation model predicts the maximum separation, whereas k-ω predicts the minimum separation length. Results confirmed that the shear layer between the mainstream and the coolant flows is the main source of turbulence generation. Ferguson et al. [7] investigated the performance of three different turbulence models combined with three different wall treatments in simulating film cooling flow on a flat plate and compered the results with an experimental database. It was found that the standard *k-ε* turbulence model was best in predicting the trend in effectiveness in the near field region and the turbulence levels within the cooling hole. It was found that the two-layer wall treatment is essential in capturing the separation bubble that is present when the coolant lifts-off the flat plate surface and then reattaches to it.

Yavuzkurt and Hassan [8] used numerical investigation to study the film cooling over flat plate with row of cylindrical cooling holes to study the performance of four turbulence models available in the commercial CFD solver FLUENT. The standard *k-ε* model yielded the best effectiveness predictions when high mainstream turbulence levels were applied at low blowing ratios. While the RNG and realizable *k-ε* models yielded similar results, they deviated from the experimental data by up to 60%.; the trend of the data was not matched at all. The standard *k-ω* model, consistently under-predicted the cooling performance and deviated from the data by up to 70%. At higher blowing ratios, all models failed to predict the cooling performance.

Harrison and Bogard [9] studied the performance of three different turbulence models (the standard *k-ω* model, the realizable *k-ε*, and the RSM model) in predicting film cooling flow behavior over a flat plate. They noted that the laterally averaged adiabatic effectiveness was best predicted with the standard *k-ω*, while centerline adiabatic effectiveness was best predicted with the realizable *k-ε* the. All models predicted poorly the lateral spreading of the coolant. They concluded that the best turbulence model must be determined based on the application that is being considered.

3. Computational Methodology

The software program GAMBIT 2.4.6 has been used to model the computational domain and to generate the mesh.

3.1 Computational Domain

The computational domain for this study matched the experimental test case of Kohil and Bogard [1]. The solid model of the whole assembly is shown in figure (1). The computational domain included the cylindrical cooling hole, and the main channel (cross hot flow). The diameter of the film cooling hole was 11.1 mm and had a length-to-diameter ratio L/D = 2.8 with an injection angle of 35^{o}. The cross flow test section was 33.3 mm in width to simulate holes spacing P/D = 3 in the actual experimental test case and 166.5 mm in height with H/D =15.

The origin of coordinate system is located at the trailing edge of the flat plate along the rare boundary of the domain in all cases at a distance of 210.9 mm (19D). An outlet boundary was imposed at 333 mm (30D) downstream of the cooling hole centerline.

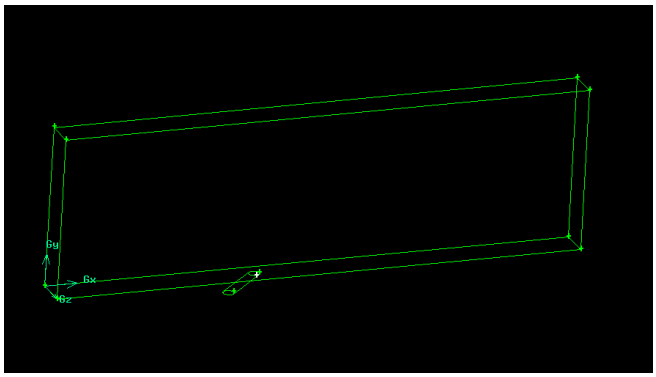

Figure (1): The computational domain

3.2 Mesh Generation

The mesh is generated using GAMBIT 2.4.6 as a pre-processor and mesh generator.
The quality of a computational solution is strongly linked to the quality of the grid mesh. So, a highly orthogonalized, nonuniform, multi-block fine grid mesh was generated with grid nodes considerably refined in the near-wall region vicinity.

The grid generated is composed of four blocks, which are:

- The first block; the domain over the cooling hole extends for 1.5D downstream and upstream the cooling hole centerline.
- The second block; the domain extends from the main flow inlet section to the first block,
- The third block; the domain extends from the 1st block to the outlet section
- The fourth domain; the domain includes the injection tube.

A fine grid mesh was generated with grid nodes considerably refined in the first block and near-wall region vicinity. The hexahedral/wedge mesh was used of cooper type for the 1st and 4th blocks and hexahedral/map mesh for the 2nd and 3rd blocks as shown in figure (2).

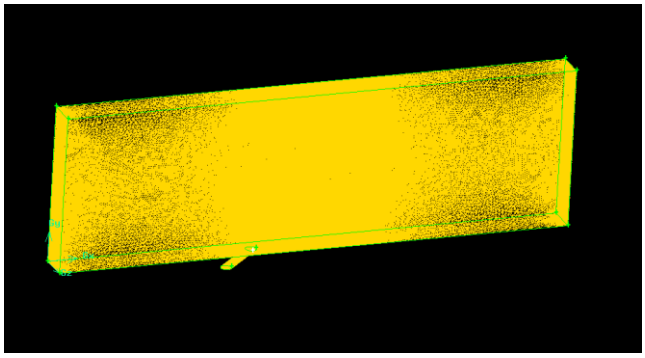

Figure (2): The generated mesh

3.3 Grid Sensitivity

A grid sensitivity test was carried out. The case for blowing ratio M=0.5 is selected. Different meshes have been tried. Figure (3) shows the mesh dependency for centerline effectiveness. The different grid sizes for various meshes are tabulated in the Table (1). From figure (3) it is clear that the result in cases of mesh 3 and mesh 4 are similar, so mesh 3 is used for analysis in the rest of this work.

Table (1)

Grid	Cells	Faces	Nodes
Mesh 1	345298	987500	305943
Mesh 2	401101	1224628	424599
Mesh 3	538475	1643141	566592
Mesh 4	601498	1834034	631467

3.4 Boundary Conditions

Boundary conditions are prescribed at all boundaries of the computational domain by imposing exactly the parameters used in the experimental work [1].

- **Main stream inlet**: The main stream gases are approximated as air, with a temperature of 300 K and has a velocity of 20 m/s and turbulent intensity of 0.2 % , and the mainstream Boundary condition is specified as “inlet velocity”.
- **Coolant inlet**: The coolant inlet is taken to be air, with a temperature of 188 K and velocity of 6.25 m/s and turbulent intensity of 0.2 %, density ratio is maintained at 1.6, and the mainstream boundary condition is specified as “inlet velocity”.
- **Flat plate**: The flat plate surfaces upstream and downstream of the hole injection are considered thermally adiabatic and the no-slip condition with wall function approach.
- **Coolant pipe walls:** The internal pipe walls of the coolant pipe are considered thermally adiabatic and the no-slip condition with wall function approach.
- Symmetry boundary conditions are used for the two lateral planes in the left and right of the computational domain. The top surface for the domain, being sufficiently far from the test plate, is also considered as symmetry plane.
- The coolant inlet velocity and temperature were kept the same in all cases which are 6.25 m/s and 188 K respectively. The coolant flow rate was altered to change the blowing ratio in such a way to be fully consistent with the procedure described by Bogard et al [1].
- **Convergence** was considered to be achieved when the residuals values were less than 10^{-4} for the continuity equation, 10^{-4} for the momentum equations, 10^{-7} for the energy equation and 10^{-3} for the turbulent kinetic energy and turbulent dissipation rate.
- **Solver**: **FLUENT** is used to simulate film cooling for the computational domain.
- **The numerical procedure** used to calculate the test case is based on a finite-volume approach. A pressure based, implicit and steady solver was used. The pressure-velocity coupling is achieved using the SIMPLE algorithm. The second order upwind scheme is chosen for the discretization of the momentum, turbulent kinetic, turbulent dissipation rate equations while first order upwind scheme was chosen for the energy equation.

3.5 CFD Validation

The experimental work of Bogard et al. [1] was chosen as the benchmark cases in order to validate the numerical methodology which is used in the paper, as well to validate the selected turbulence model.

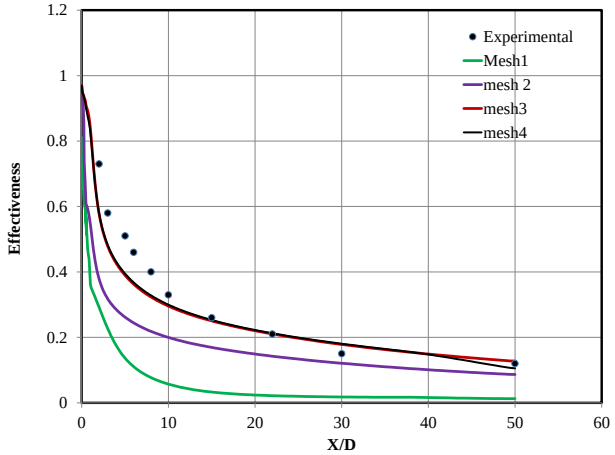

Figure (3): Central line effectiveness for different generated grid
(Grid sensitivity analysis)

4. Results and Discussions

4.1 Effect of Wall Treatment

Figure (4) shows a comparison between the experimental data of Bogard et al [1] and predicted centerline film cooling effectiveness for two different wall functions at the blowing ratios of 0.5 and 1 when standard k–ε model was used to model the flow. Moreover, the realizable k–ε model combined with the standard wall and the enhanced wall treatment (two-layer approach) are shown in figure (5). The two cases were used to investigate the influence of near-wall modeling on the centerline film cooling effectiveness at different blowing ratios and coolant injection angles.

It can be concluded that both wall treatments results were in good agreement for all the studied cases when standard k–ε model was used at lower blowing ratio M=0.5. This may be attributed to the good fine mesh generated near the wall in the computational domain. Realizable k–ε model with enhanced wall treatment may be recommended for high blowing ratios.

4.2 Effect of Turbulent Models

Five different turbulence models were investigated: the k- ε models (standard, RNG and realizable), and k- ω models (standard and the Shear Stress Transport (SST) model)

The performance of these models was evaluated for blowing ratios of 0.5 and 1, with injection angles of 35^o and 55^o as shown in Figures (6-9).

The turbulent models are applied to model the flow field. Although the they have a good trend for centerline film cooling effectiveness at the low blowing ratio of 0.5, they are not able to predict the experimental results in the region of 3 < X/D < 10 for injection angle of 35^o as shown in figure (6). At a higher injection angle, all turbulent models are in agreement with experimental results for whole range of X/D. However, a small enhancement was noticed when using realizable and RNG k-ε model compared with both k-ω models as shown in figure (7).

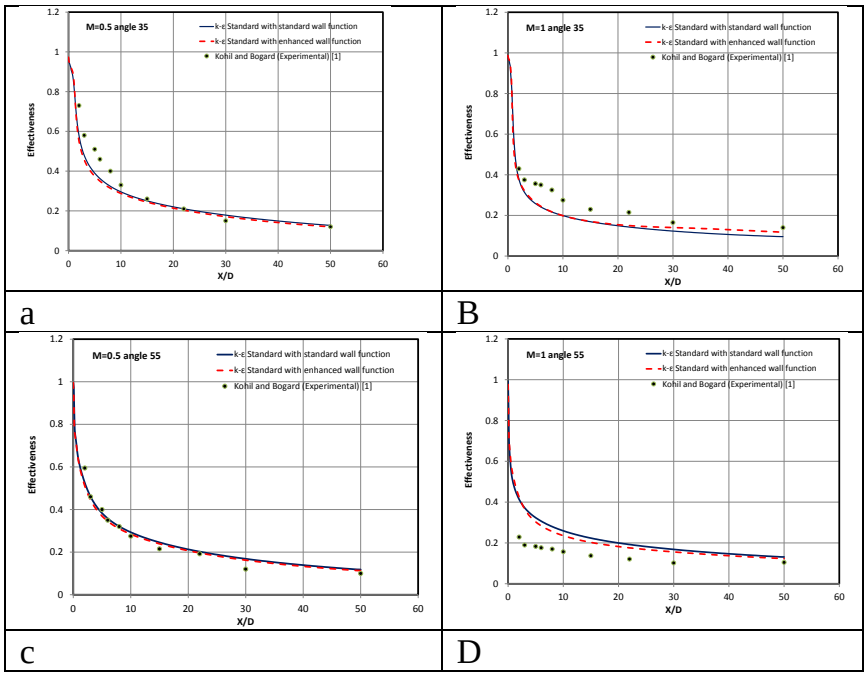

Figure (4): Comparison between numerical results of k–ε standard model with two different wall functions, and the experimental results.

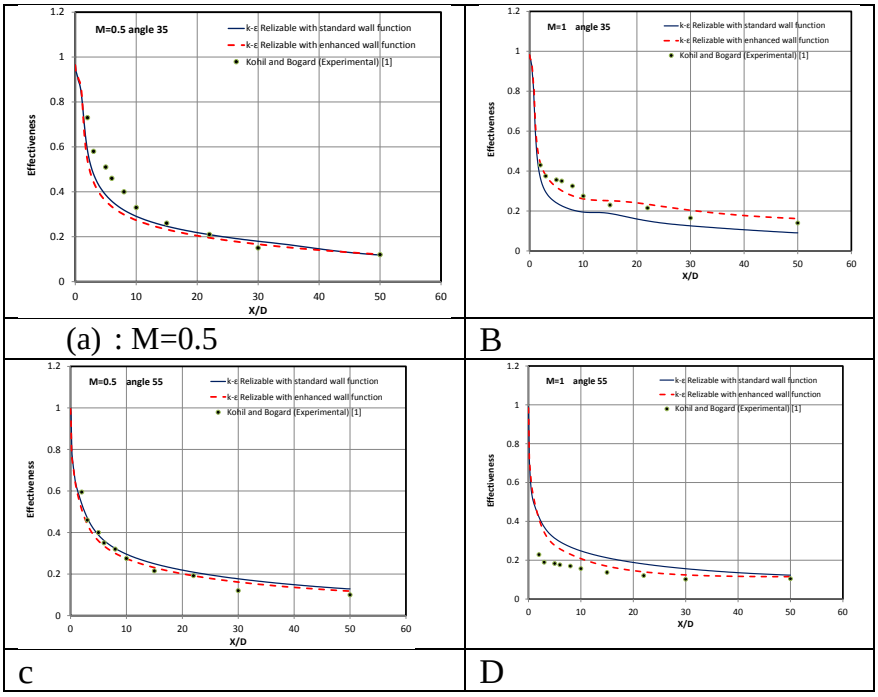

Figure (5): Comparison between numerical results of k–ε realizable model with two different wall functions, and the experimental results.

At high blowing ratio (M=1), for injection angle 35^o, the turbulent model RNG k–ε was not able to capture the jet lift-off effect in the near hole region of x/D < 5. This may be attributed to the fact that the flow field in the near hole region is highly swirling. However, it had an excellent trend for 5 < X/D < 50. Realizable k–ε provides a good trend for the entire range of X/D. On the other hand, the other turbulence models, such as the standard and k-ω model, are performing better in this region X/D <5 as shown in figure (8).

For injection angle 55^o all turbulent models were not able to capture the jet lift-off effect in the near hole region of x/D < 10. Based on this observation, with higher blowing ratios and higher injection angles one may predict a higher jet lift-off effect. In the far field region realizable model was performing better than the other with acceptable differences as shown in figure (9).

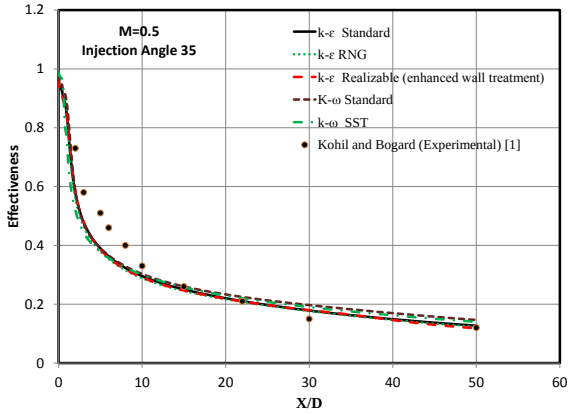

Figure (6): Effect of turbulent models at injection angle of 35° and blowing ratio of 0.5.

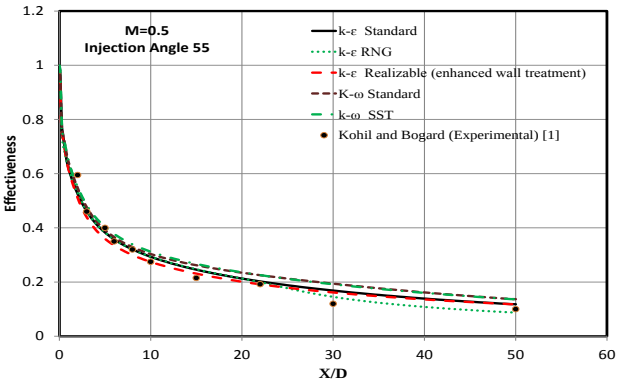

Figure (7): Effect of turbulent models at injection angle of 55° and blowing ratio of 0.5

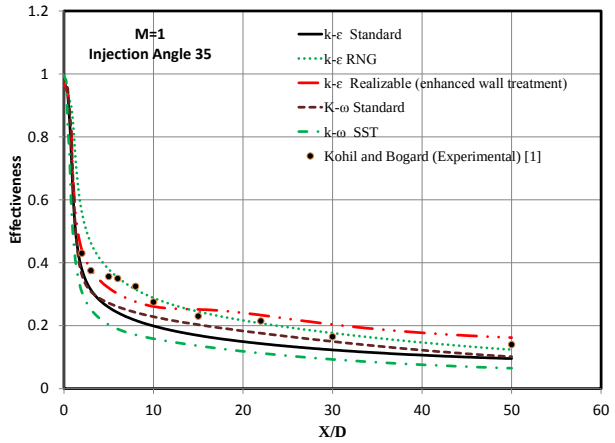

Figure (8): Effect of turbulent models at injection angle of 35° and blowing ratio of 1.

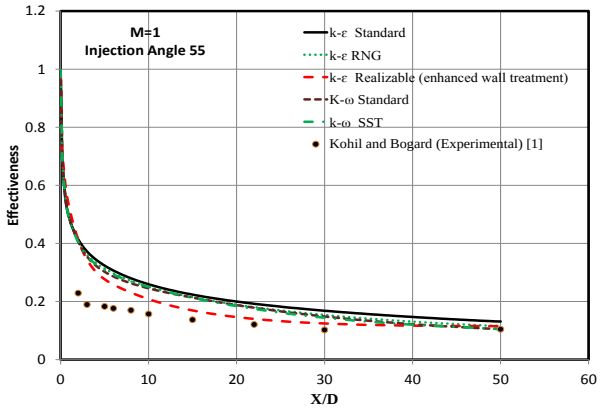

Figure (9): Effect of turbulent models at injection angle of 55° and blowing ratio of 1.

In general, the realizable k–ε model outperforms all other tested turbulence models. The deviation of the predicted results with the other models from the experimental data is more than that with the realizable k–ε model in the downstream region (x/D > 10). Generally speaking, the realizable k–ε model was in reasonable agreement with experimental data and performed better, compared with other turbulence models; hence, the rest of calculations were carried out with this model combined with the enhanced wall function. This result agrees with the study results obtained by Harrison and Bogard [9], Khajehhasani [10] and Silieti et al. (2009b) [11].

4.3 Effect of Injection Angle

As film cooling research has mainly focused on studying holes with injection angles of about 30°, there is a dearth of studies investigating large injection angles [1]. The motivation for this study was to determine the sensitivity to injection. In this section detailed effectiveness, thermal and velocity field predictions for round holes with an injection angle of 35° and 55° were conducted.

Centerline effectiveness as a function of stream wise distance for the 35° and 55° holes at low and high blowing ratios are presented in Figures (10) and (11). At M= 0.5, the centerline effectiveness of the 55° holes is only slightly inferior to the 35° holes, This results agree with previous work carried out by Bogard et al [1]. But at M = 1, Bogard et al [1] concluded that there is a significant reduction in centerline effectiveness for the 55° holes which is clear in results shown in figure (11).

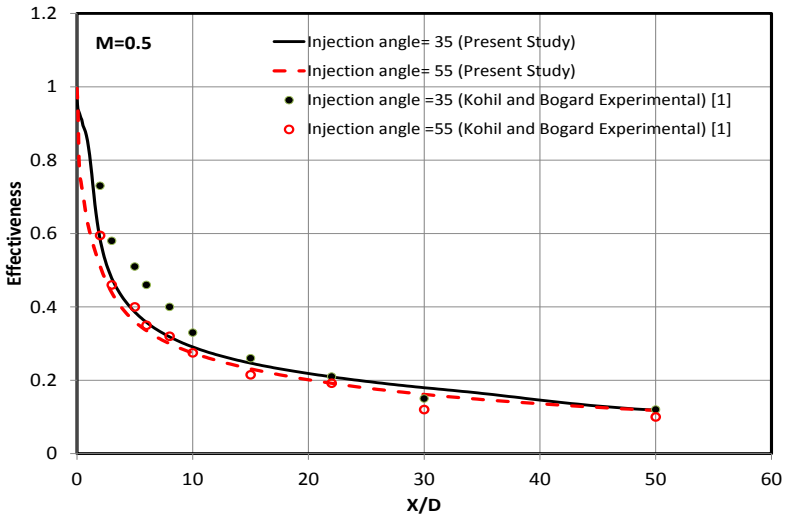

Figure (10): Comparison of centerline effectiveness for the 35° and 55° round holes at low blowing ratio M=0.5.

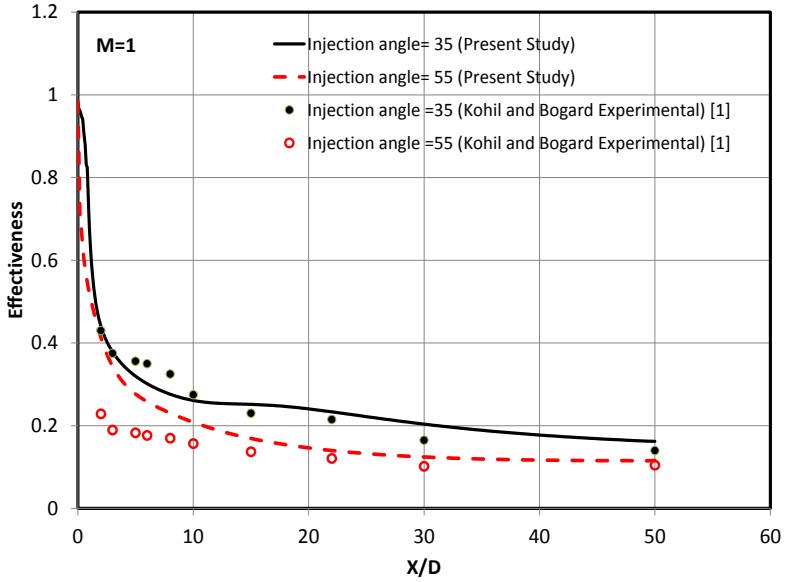

Figure (11): Comparison of centerline effectiveness for the 35° and 55° round holes at high blowing ratio M=1.

Figure (12) shows the mean velocity contours near the injection location for the 35º and 55º injection angles for M=0.5. At injection angle of 35º the free stream pushes the jet towards the wall, bending the jet over completely by *xlD* = 3. It is clear from the velocity contours, that there is slight separation region at *x/D* < 3. At Higher injection angle of 55º, more cooling jet penetration was noticed, leading to an increase of the separation region to X/D ≈5.

In the case of the high blowing ratio M=1, as shown in figure (13), the velocity contours indicate an upward motion at (Xl D = 1) in both injection angles. However, this upward motion seems to be stronger with higher injection angle. Figure (14) shows the effectiveness contour for the 35° and 55º holes and blowing ratio of 0.5 at the jet centerline near the injection location. The effectiveness contours over the hole indicate that at this blowing ratio, $\eta \geq 0.9$ at X/D= 1 for the injection angle of 35º compared with about $\eta = 0.7$ at the same location for injection angle of 55º. Also, for injection angle 35º, there are no levels higher than $\eta = 0.5$ beyond x/D = 3 while compared with X/D =2 for injection angle of 55º. These results support the view point that there is a jet lift off at higher injection angle.

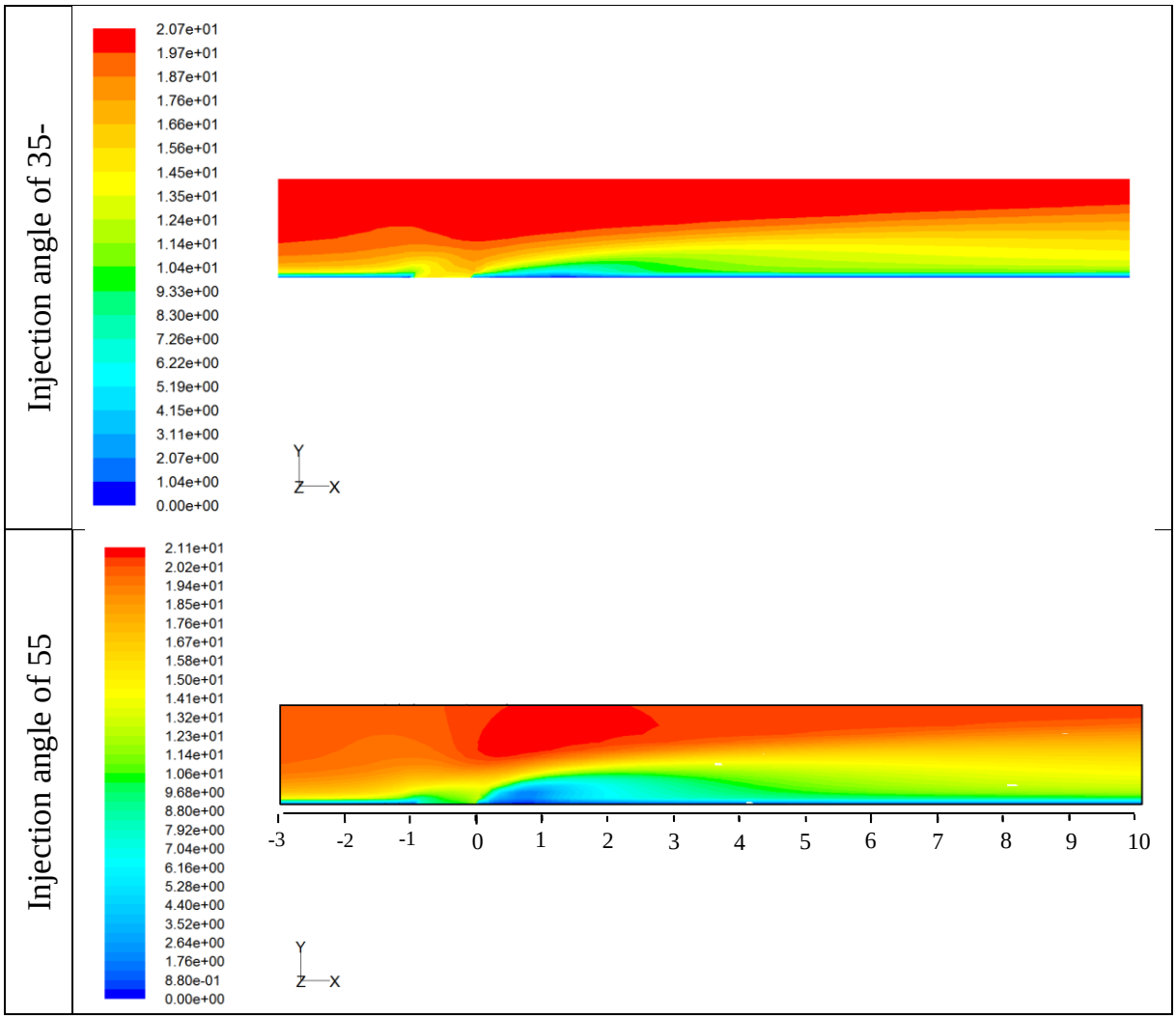

Figure (12): The mean velocity contours near the injection location for the 35º and 55º injection angles for M=0.5

For comparison, Figure (15) shows the effectiveness contours for 35° and 55° round hole at a higher blowing ratio of 1. The most distinctive difference between the M=0.5 and M=1 cases is the significantly greater jet penetration of the cooling jet, which increases with higher injection angle. For M=1, there are no levels higher than η = 0.5 beyond x/D = 1.5 compared with X/D =1 at higher injection angle.

Figures (16) and (17) show the detailed adiabatic wall film cooling effectiveness distributions for the flat plate at injection angles of 35° and 55° at M =, 0.5 and 1 respectively. At a blowing ratio, M=0.5 there was no jet lift off was noticed which appear in the region in which the effectiveness contours for η = 0.7 curve was located near the hole exit at almost X/D ≈ 2 compared with X/D ≈1 at higher injection angle. However, the centerline effectiveness increases to 0.98 at X/D=0 due to increase of flow momentum. Under a higher blowing ratio, M=1, the coolant jet appeared to lift off at the down- stream edge of film holes and reattach further down- stream. This created a higher temperature region just downstream of the holes where the effectiveness was found to be 0.98 at X/D=0 for injection angle of 35° as shown in figure (17).

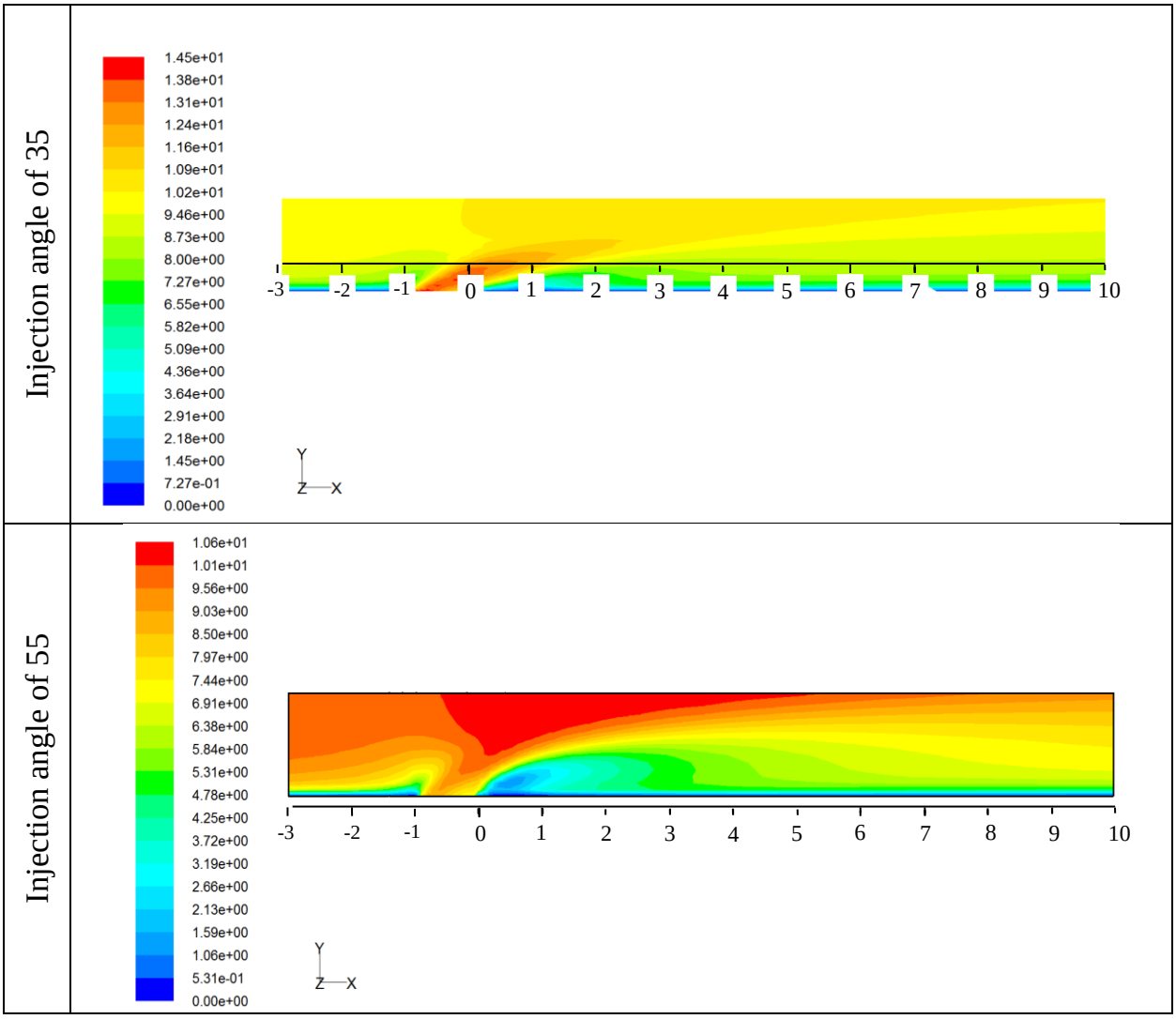

Figure (13): The mean velocity contours near the injection location for the 35° and 55° injection angles for M=1

The coolant jet lifts off from the wall. The effectiveness contours for η = 0.6 curve was located near the hole exit at X/D = 1 compared with X/D = 0.5 at higher injection angle at the same location. The centerline effectiveness was shown to decreases dramatically downstream the trailing edge of the cooling jet as shown at X/D=1at which the effectiveness was found to be 0.6 at 35o injection angle compared with 0.5 at the same location for 55º injection angle.

Effectiveness contours, η, of the film cooling jet in the lateral plane at x/D = 0, 3, and 6 for both injection angles 35º and 55º at two blowing ratios (M=0.5 and M=1) were shown in Figure (18) and (19) respectively. The height of each section presented is y=1.5D while the width of the section extends to right and left from the test plate center line from Z/D=0.0 to Z/D =±1.5 D. At x/D = 0, the jet is already diffuse because of interaction with the mainstream. This is illustrated by the η = 0.9 contour which is limited to a very small region at the core of the jet at injection angle of 35º and X/D=0. This region was shown to increase for the same location due to higher jet penetration at higher injection angle 55º. The reduction in contour levels indicates the drop in effectiveness which occurs as the jet moves downstream. The values of η = 0.1 occurs at Y/D=1.2 at X/D = 6, and slightly increases with higher injection angle at M=0.5 as shown in figure (18).

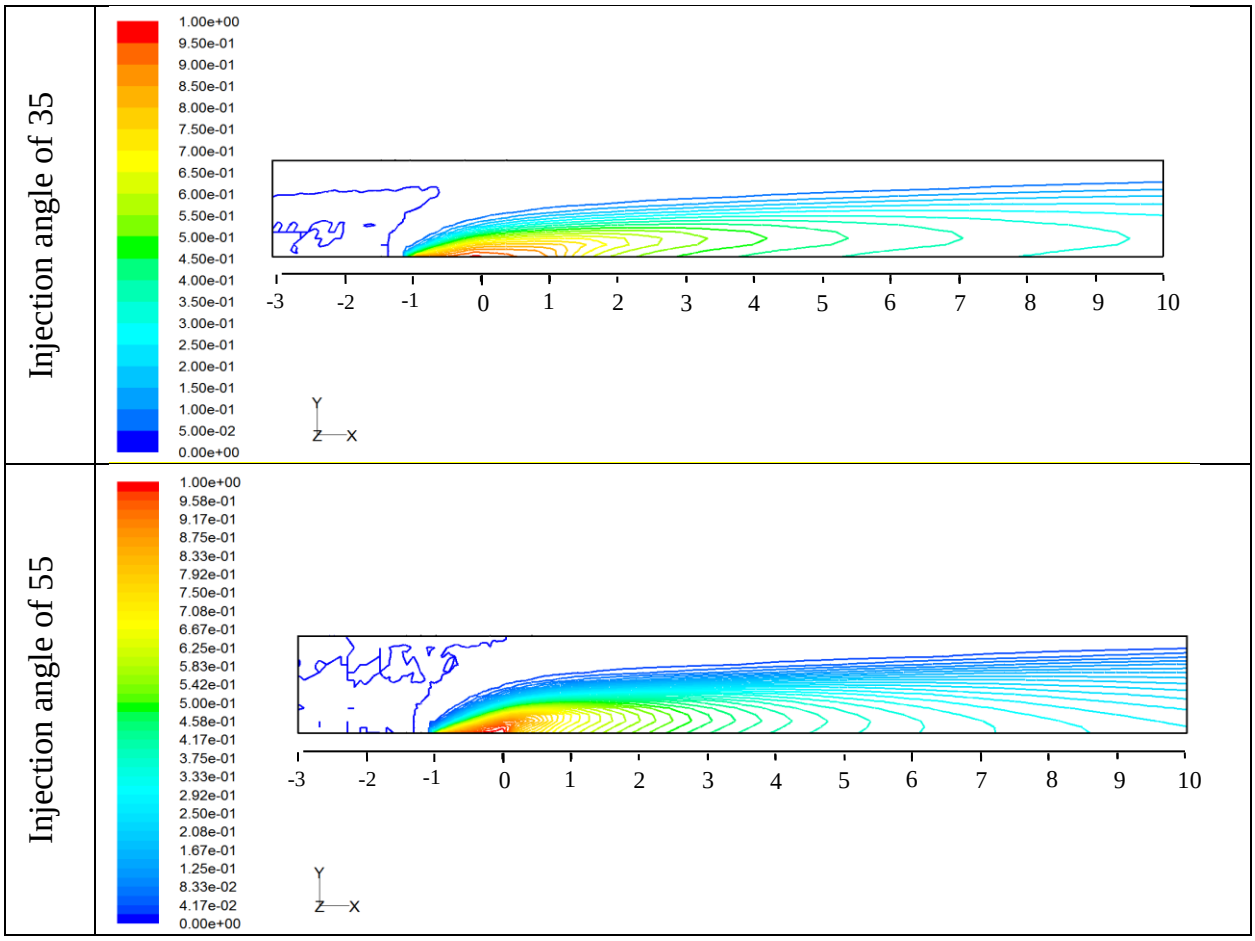

Figure (14): The effectiveness contour for the 35° and 55º holes and blowing ratio of M=0.5.

The cooling jet penetration through the main flow is more obvious at higher blowing ratio of M=1 especially at 55º injection angle. The values of high effectiveness contours of η = 0. Extended to a higher Y/D ratio at higher injection angle for X/D =0. The height at which maximum effectiveness contours were located were always at higher Y/D as the blowing ratios increases at different values of X/D. This increase in effectiveness is useless because it occurs away from the test plate.

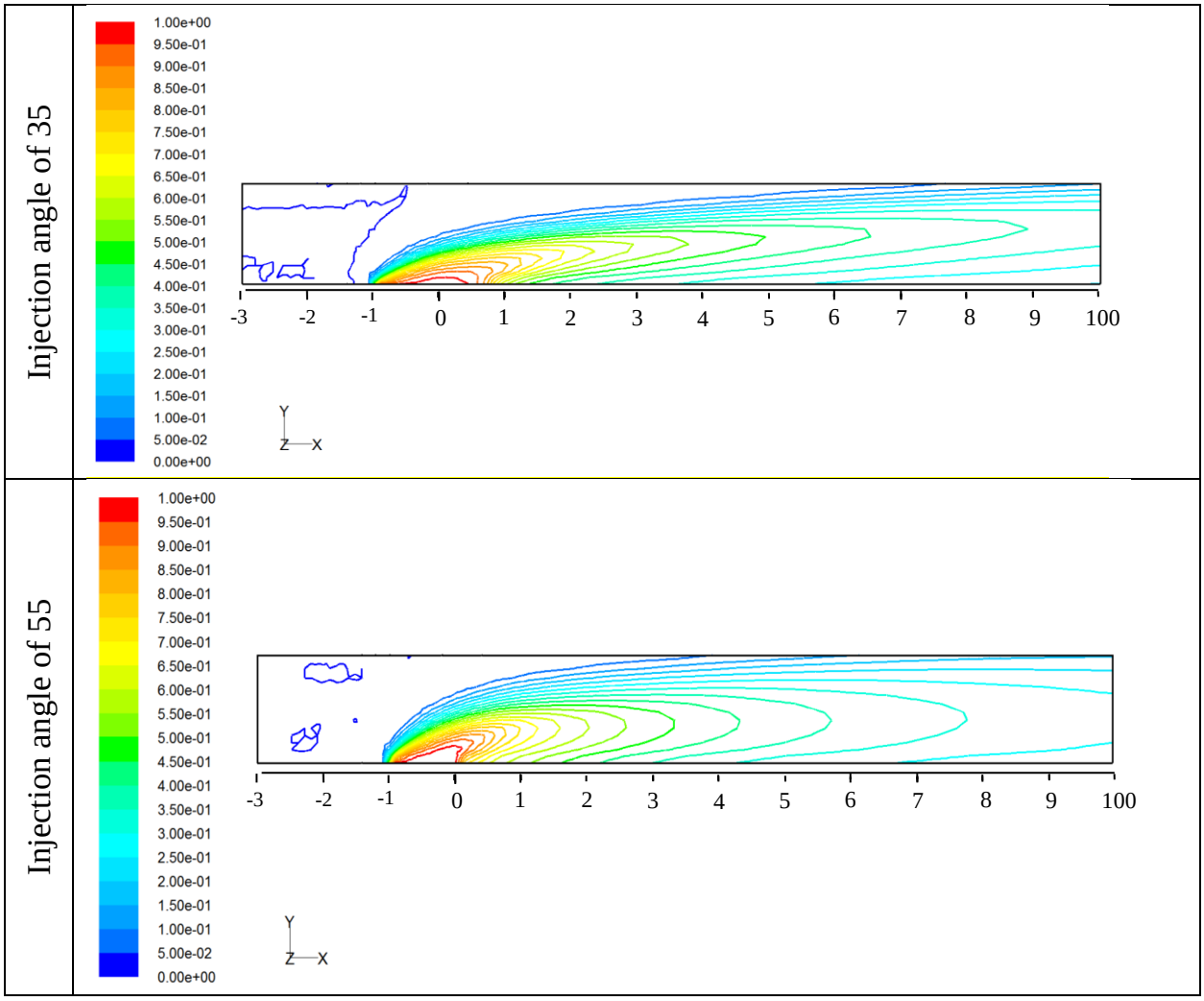

Figure (15): The effectiveness contour for the 35° and 55º holes and blowing ratio of M=1

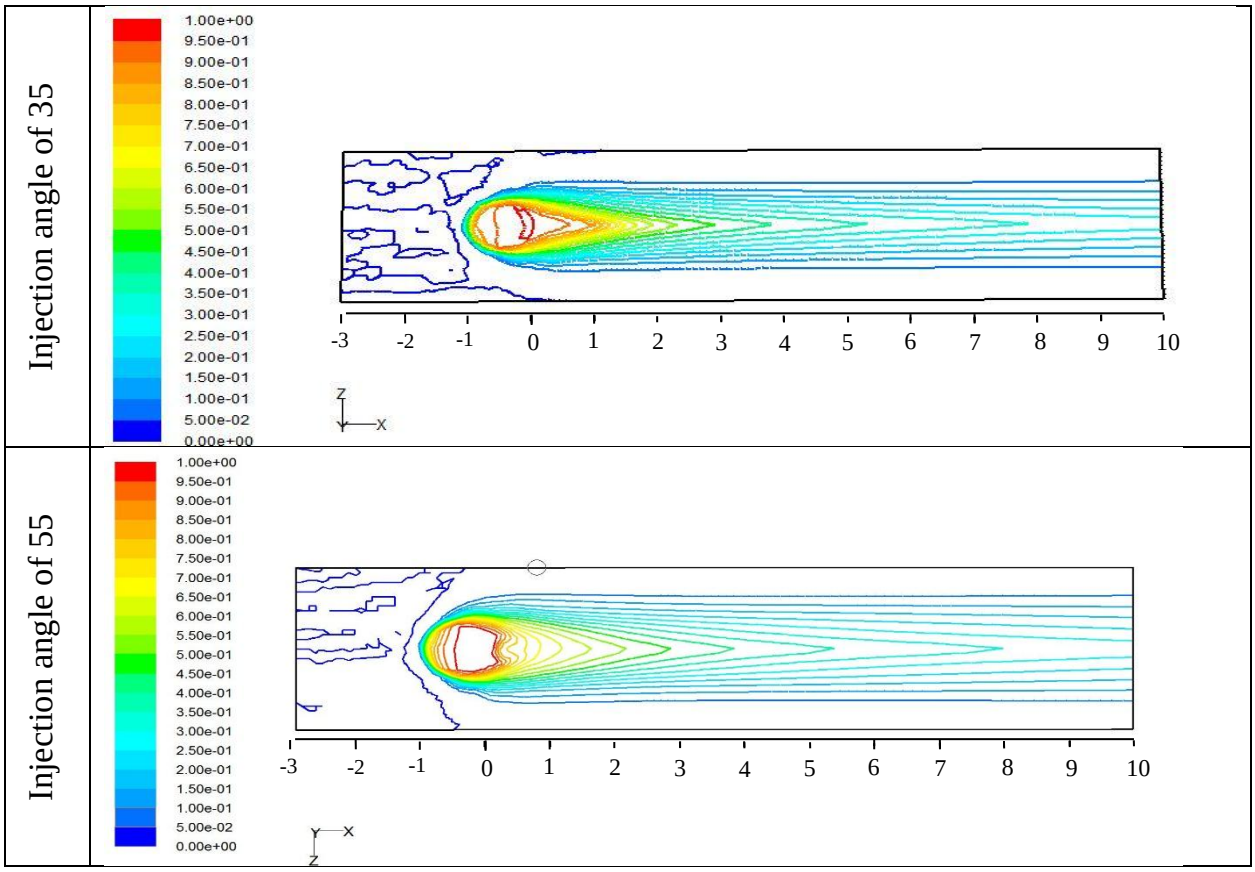

Figure (16): The detailed adiabatic wall film cooling effectiveness distributions for the flat plate at injection angles of 35° and 55° at M = 0.5.

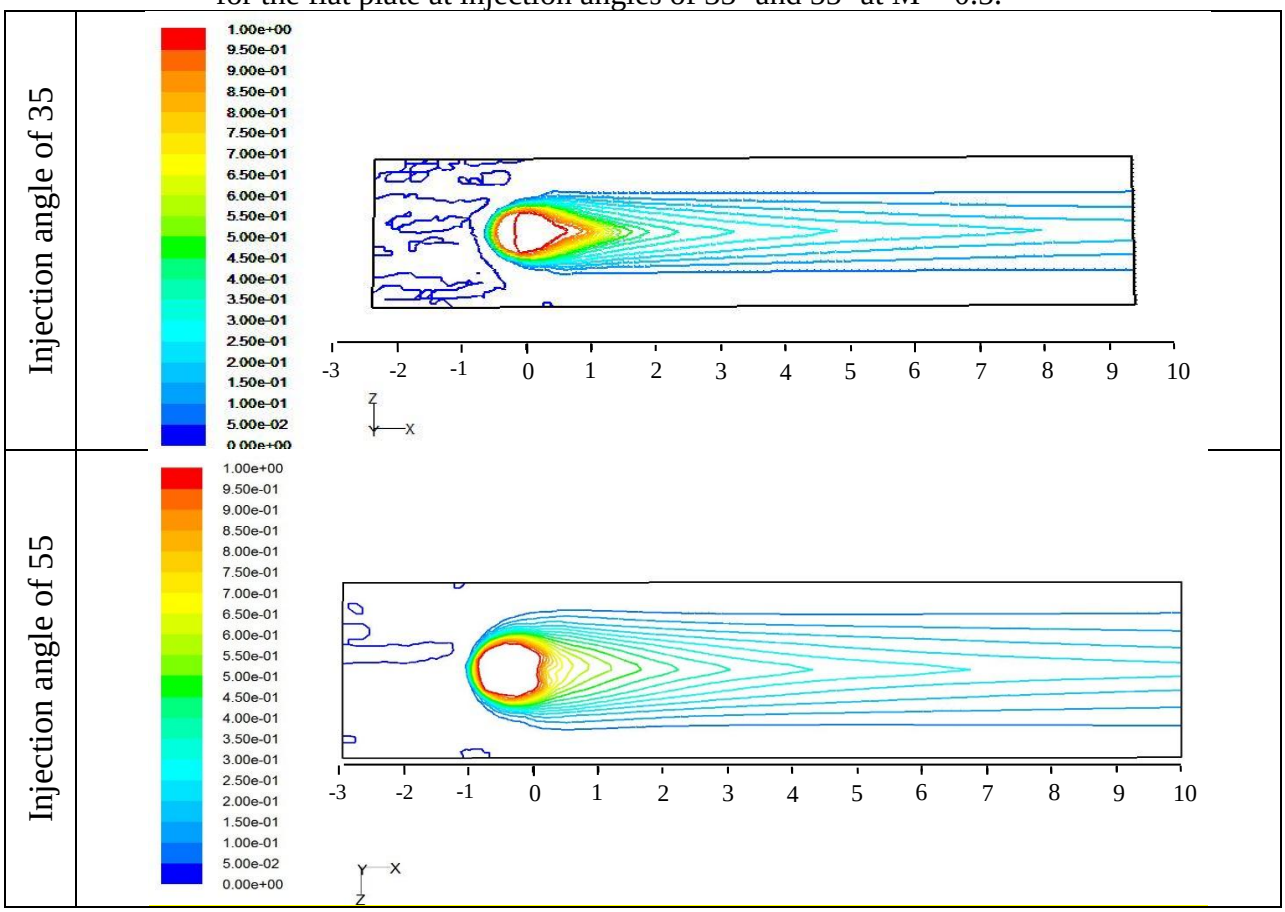

Figure (17): The detailed adiabatic wall film cooling effectiveness distributions for the flat plate at injection angles of 35° and 55° at M=1

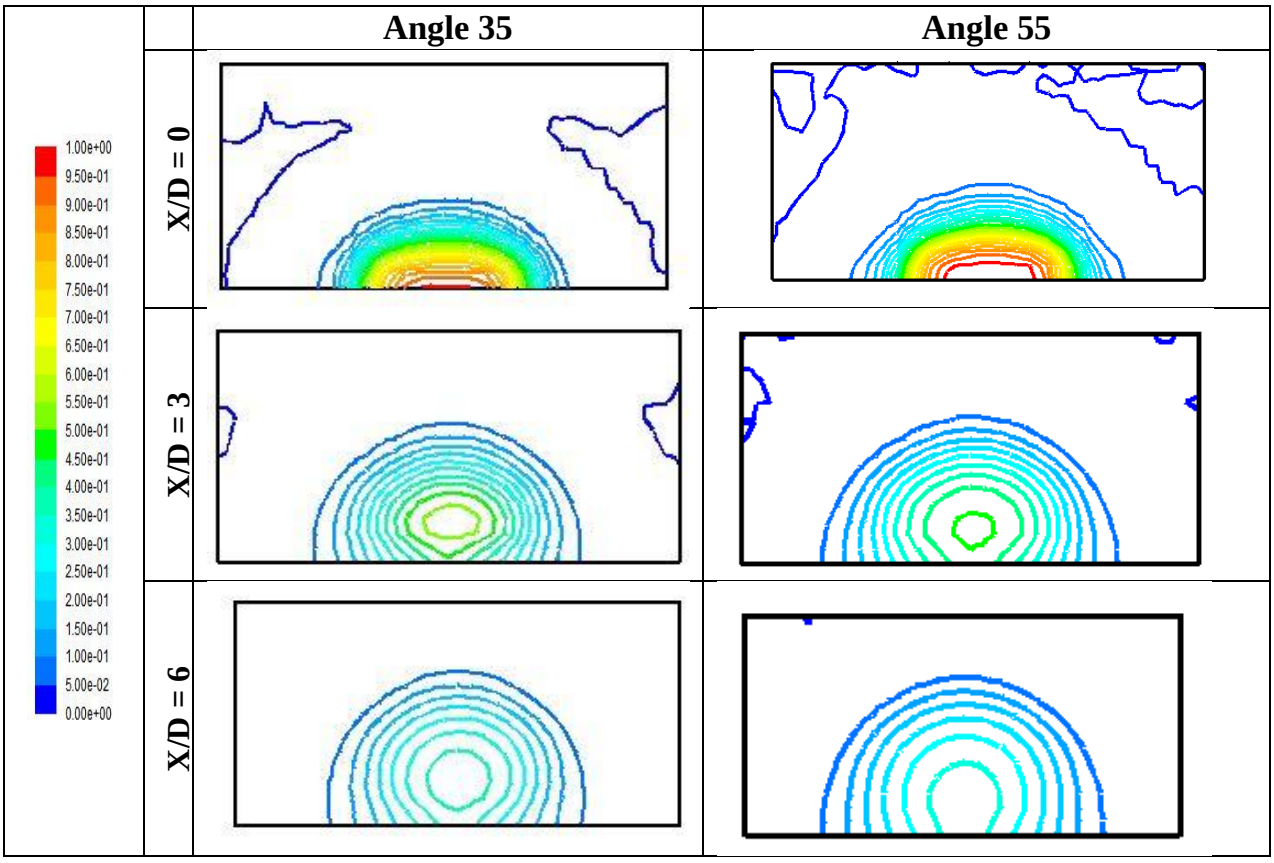

Figure (18): Effectiveness contours of the film cooling jet in the lateral plane at x/D = 0, 3, and 6 for both injection angles 35° and 55° at blowing ratio of M=0.5.

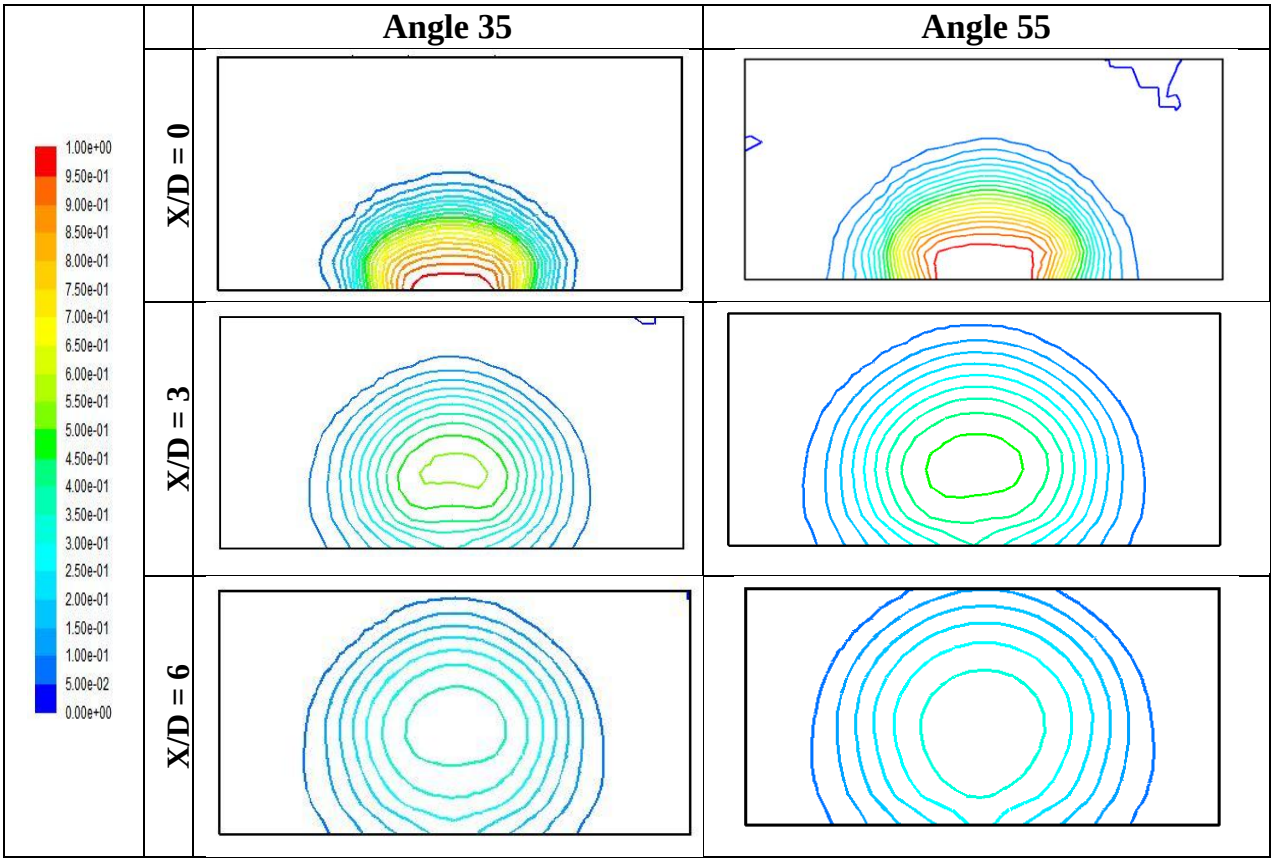

Figure (19): Effectiveness contours of the film cooling jet in the lateral plane at x/D = 0, 3, and 6 for both injection angles 35° and 55° at blowing ratio of M=1

5. Conclusions

The following are the summary of the most important concluding remarks from the present study

- Realizable k–ε model with enhanced wall treatment was recommended for high blowing ratios.
- No specific turbulence model was found fit to be generalized to all blowing ratios
- Increasing in injection angle, Leeds to a reduction in film effectiveness. This may be attributed to the fact that, there is a greater tendency for coolant jet separation at higher injection angle which causes lower film effectiveness.

6. References

1. - Kohli, A., and Bogard, D., "Adiabatic Effectiveness, Thermal Fields, and Velocity Fields for Film Cooling with Large Angle Injection," *Journal of Turbomachinery*, Vol. 119, 1997, pp. 352–358.
2. Han J-C, Dutta S, Ekkad SV (2000) Gas turbine heat transfer and cooling technology. Taylor and Francis Publications, New York.
3. Foster, N.W., and Lampard, D., "The Flow and Film Cooling Effectiveness Following Injection Through a Row of Holes Journal of Engineering for Power, Vol. 102, 1980, pp. 584–588.
4. Baldauf, S., Scheurlen, M., Schulz, A., and Wittig, S., "Correlation of Film-Cooling Effectiveness from Thermographic Measurements at Enginelike Conditions," Journal of Turbomachinery, Vol. 124, 2002, pp. 686–698.
5. Amer, A.A., Jubran, B.A. and Hamdan, M.A., Comparison of Different Two-Equation Turbulence Models for Prediction of Film Cooling from Two Rows of Holes. Numerical Heat Transfer, Part A: Application: An Internation Journal of Computation and Methodology, 1992.
6. Sarkar, S. and Bose, T.K., Comparison of Different Turbulence Models for Prediction of Slot-Film Cooling: Flow and Temperature Field, Numerical Heat Transfer, Part B, 1995.
7. Bc- Ferguson, J.D., Walters, D.K. and Leylek, J.H., Performance of Turbulence Models and Near-Wall Treatments in Discrete Jet Film Cooling Simulations, 1998.
8. Yavuzkurt, S. and Hassan, J.S., Evaluation of Two-Equation Models of Turbulence in Predicting Film Cooling Performance under High Free Stream Turbulence, 2007.
9. Harrison, K.L. and Bogard, D.G., Comparison of RANS turbulence models for prediction of film cooling performance, 2008.
10. Siavash Khajehhasani "NUMERICAL MODELING OF INNOVATIVE FILM COOLING HOLE SCHEMES
11. Silieti, M., Kassab, A.J. and Divo, E., Film cooling effectiveness: Comparison of adiabatic and conjugate heat transfer CFD models, International Journal of Thermal Sciences, 48:2237-2248, 2009b.